

Article

Magnetocaloric Properties of $(\text{MnFeRu})_2(\text{PSi})$ as Magnetic Refrigerants near Room Temperature

Takayuki Ohnishi ¹, Kei Soejima ¹, Keiichiro Yamashita ¹ and Hirofumi Wada ^{2,*}

¹ Research & Development Group, Dyden Cooperation, Kamimine-cho, Miyaki-gun, Saga 849-0124, Japan; oonishi@dyden.co.jp (T.O.); kei_soejima@dyden.co.jp (K.S.); yamashita@dyden.co.jp (K.Y.)

² Department of Physics, Kyushu University, Motoooka 744, Nishi-ku, Fukuoka 819-0395, Japan

* Correspondence: wada@phys.kyushu-u.ac.jp; Tel.: +81-92-802-4073

Academic Editor: Adriana Greco

Received: 13 January 2017; Accepted: 27 January 2017; Published: 8 February 2017

Abstract: We have scaled up the production process of magnetic refrigerants near room temperature. The $\text{Mn}_{2-y}\text{Fe}_y\text{Ru}_x\text{P}_{1-z}\text{Si}_z$ compounds with $0.03 \leq x \leq 0.16$, $y \approx 0.75$, and $z \approx 0.55$ were synthesized and their magnetocaloric properties were examined. By changing the compositions and the annealing temperature, the Curie temperature was tuned between 275 and 315 K with 2–3 K steps. All the compounds underwent a first-order magnetic transition accompanied by thermal hysteresis of less than 2 K. The compounds showed excellent magnetocaloric properties: the magnetic entropy change was more than 10 J/K·kg and the refrigerant capacity was about 115 J/kg in a field change of 1.5 T. The detailed instructions to synthesize high-performance $(\text{MnFe})_2\text{PSi}$ materials are given.

Keywords: magnetocaloric effect; magnetic refrigeration; first-order magnetic transition; magnetic entropy

1. Introduction

About 40 years ago, Brown reported the first demonstration of magnetic cooling near room temperature [1]. Since then, considerable effort has been devoted to developing magnetic refrigeration systems. Magnetic refrigeration is based on magnetocaloric effects (MCEs), which mean changing the entropy or temperature of magnetic materials by applying/removing the magnetic field. Since this technology is environmentally friendly and highly energy-efficient, magnetic refrigeration is expected to be an alternative cooling technology to conventional gas compression systems in the near future. To realize magnetic refrigeration systems, materials exhibiting large MCEs are strongly desired. Some ferromagnetic materials are known to undergo a first-order magnetic transition (FOMT) at the Curie temperature, T_C , and show giant MCEs near room temperature. Typical examples are $\text{Gd}_5\text{Si}_2\text{Ge}_2$ [2], $\text{MnAs}_{1-x}\text{Sb}_x$ [3], $\text{MnFeP}_{1-x}\text{As}_x$ [4], $\text{La}(\text{Fe}_{1-x}\text{Si}_x)_{13}\text{H}_y$ [5], and NiMnSn Heusler alloys [6]. These materials are potential candidates for magnetic refrigerants. Note that, except $\text{Gd}_5\text{Si}_2\text{Ge}_2$, these candidates are 3d transition metal-based compounds. Among them, $\text{Mn}_{2-y}\text{Fe}_y\text{P}_{1-z}\text{Si}_z$, which is a derivative system of $\text{MnFeP}_{1-x}\text{As}_x$, is one of the most promising materials near room temperature, because it consists of nontoxic and inexpensive elements and the compound is very stable in water as well as in air. This system has a hexagonal Fe_2P -type structure in the concentration ranges of $0 \leq y \leq 1$ and $0.28 \leq z \leq 0.64$. The structure has two chemical sites for transition metals, 3g and 3f. Neutron diffraction studies have revealed that Mn atoms preferentially occupy the 3g site, while Fe atoms occupy the 3f site [7]. In 2008, Cam Thanh et al. succeeded in preparing $\text{Mn}_{2-y}\text{Fe}_y\text{P}_{1-z}\text{Si}_z$ with the Fe_2P -type structure for the first time [8]. They found that the compounds with $y = 1$ and $z \approx 1$ undergo a FOMT and exhibit giant MCEs near room temperature. However, these compounds have a large thermal hysteresis, ΔT_{hys} , of 20–30 K, which is unfavorable for magnetic refrigeration materials. Subsequent work reported that heat treatment does not improve the hysteretic behavior [9]. Therefore,

it is necessary to change the compositions or to dope guest elements for the reduction of ΔT_{hys} without losing the giant MCEs. Dung et al. successfully reduced ΔT_{hys} by choosing $y = 0.7\sim 0.8$ [10]. On the other hand, we reported that the Ru substitution in $Mn_{2-y}Fe_yP_{1-z}Si_z$ is effective to reduce ΔT_{hys} [11]. A similar doping effect was also reported for Co and Ni substitutions [12]. One of the advantages of the Ru-substituted system is the moderate change of T_C with the Ru content. We have shown that T_C of the materials can be tuned to the desired temperature by changing the Ru content.

For practical applications, it is important to develop the production process at an industrial scale. For this purpose, we constructed an electric furnace, the tube of which is made of stainless steel with a diameter of 100 mm [13]. This furnace enables us to synthesize plate-type materials up to 250 g and rod-type materials up to 700 g in one batch. In this paper, we report the magnetic phase transitions and MCEs of $Mn_{2-y}Fe_{y-x}Ru_xP_{1-z}Si_z$ with $0.03 \leq x \leq 0.16$, $y \approx 0.75$, and $z \approx 0.55$ produced at an industrial scale. We have established a recipe to synthesize giant magnetocaloric materials, which have the Curie temperature of 275–315 K with 2–3 K steps.

2. Results and Discussion

We prepared a number of samples with different compositions and different heat treatments to tune T_C to 275–315 K. In this paper, we show the results of 14 samples, the compositions and sintering temperature of which are listed in Table 1. Some of them have the same compositions and the sintering temperature is different. As described in Section 3, the samples were annealed after sintering to ensure homogeneity. We found that repetitive annealing is effective to make the FOMT sharper.

Table 1. Nominal compositions and the sintering temperature of the samples synthesized in the present study. The Curie temperature, T_C , and the thermal hysteresis, ΔT_{hys} , are also listed.

Sample No.	Nominal Composition	Sintering Temp. (°C)	T_C (K)	ΔT_{hys} (K)
1	$Mn_{1.24}Fe_{0.60}Ru_{0.16}P_{0.46}Si_{0.54}$	1105	280.4	1.4
2	$Mn_{1.24}Fe_{0.62}Ru_{0.14}P_{0.46}Si_{0.54}$	1110	284.5	1.5
3	$Mn_{1.24}Fe_{0.64}Ru_{0.12}P_{0.46}Si_{0.54}$	1105	288.1	1.4
4	$Mn_{1.24}Fe_{0.64}Ru_{0.12}P_{0.46}Si_{0.54}$	1100	289.7	1.8
5	$Mn_{1.23}Fe_{0.65}Ru_{0.12}P_{0.46}Si_{0.54}$	1100	292.3	1.7
6	$Mn_{1.24}Fe_{0.67}Ru_{0.09}P_{0.46}Si_{0.54}$	1100	294.3	1.5
7	$Mn_{1.24}Fe_{0.68}Ru_{0.08}P_{0.46}Si_{0.54}$	1100	296.1	1.8
8	$Mn_{1.24}Fe_{0.68}Ru_{0.08}P_{0.46}Si_{0.54}$	1095	297.4	1.7
9	$Mn_{1.24}Fe_{0.68}Ru_{0.08}P_{0.46}Si_{0.54}$	1090	299.7	1.5
10	$Mn_{1.25}Fe_{0.70}Ru_{0.05}P_{0.46}Si_{0.54}$	1100	302.3	1.8
11	$Mn_{1.25}Fe_{0.70}Ru_{0.05}P_{0.46}Si_{0.54}$	1090	305.3	1.7
12	$Mn_{1.25}Fe_{0.71}Ru_{0.04}P_{0.45}Si_{0.55}$	1085	309.0	1.8
13	$Mn_{1.25}Fe_{0.71}Ru_{0.04}P_{0.45}Si_{0.55}$	1090	311.8	1.8
14	$Mn_{1.25}Fe_{0.72}Ru_{0.03}P_{0.45}Si_{0.55}$	1085	315.9	1.5

Figure 1a,b illustrate the DSC curves of $Mn_{1.24}Fe_{0.76-x}Ru_xP_{0.46}Si_{0.54}$. The numbers in the figure represent the sample numbers in Table 1. The solid lines are the data for the samples annealed twice and the dashed lines are for the samples annealed once. It was seen that the second annealing increased the peak height for all the samples by 10%–30%. This means that repetitive annealing improves homogeneity and it makes the magnetic transition sharper. The DSC peak position is close to the Curie temperature. The peak temperature slightly changed with additional annealing. The temperature interval between the two adjacent DSC peaks was 2–4 K. As listed in Table 1, samples 7, 8, and 9 have the same compositions. We found that the higher sintering temperature decreased T_C . A similar tendency was also observed for the other sample sets with the same compositions. Recently, Yu et al. reported the effects of heat treatment on the structure and magnetic properties of $Mn_{1.15}Fe_{0.85}P_{0.52}Si_{0.45}B_{0.03}$ [14]. They found that T_C increases with increasing the annealing temperature, which is contrary to our cases. These results suggest that the annealing temperature has a strong impact on the composition of the main phase with the Fe_2P -type structure. Höglin et al.

studied the phase diagram of $\text{FeMnP}_{1-v}\text{Si}_v$ and found that three phases coexist in the concentration range of $0.50 \leq v \leq 1.0$: the hexagonal Fe_2P -type phase, the hexagonal Mn_5Si_3 -type phase and the cubic Fe_3Si -type phase [15]. It is likely that selective diffusion between the main phase and the impurity phases or grain boundaries is responsible for the different dependence of T_C on the annealing temperature. To clarify this problem, further metallurgical studies are necessary. Our results indicate that adjusting the annealing temperature is effective to control the Curie temperature in the present system.

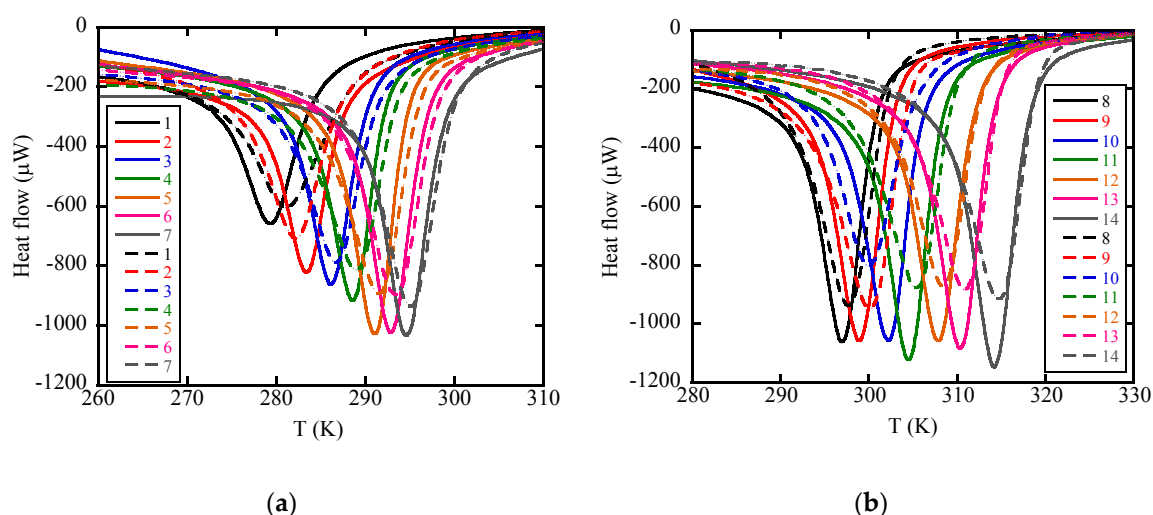


Figure 1. Differential scanning calorimetry (DSC) curves of (a) samples No. 1–7 and (b) samples No. 8–14. The numbers represent the sample numbers listed in Table 1. The solid lines represent the DSC curves measured for the samples annealed twice and the dashed lines are those for the samples annealed once. All the curves are measured in the heating process.

Figure 2 displays the temperature dependence of the magnetization of the selected samples at a magnetic field of 1 T. Both the heating and cooling processes are plotted. All the compounds undergo a FOMT accompanied by thermal hysteresis. The Curie temperature was obtained from the peak position of $dM/dT - T$ curves at 0.2 T in the heating process, which is also listed in Table 1. The Ru concentration dependence of the T_C of three series, $\text{Mn}_{1.24}\text{Fe}_{0.76-x}\text{Ru}_x\text{P}_{0.46}\text{Si}_{0.54}$, $\text{Mn}_{1.25}\text{Fe}_{0.75-x}\text{Ru}_x\text{P}_{0.46}\text{Si}_{0.54}$, and $\text{Mn}_{1.25}\text{Fe}_{0.75-x}\text{Ru}_x\text{P}_{0.45}\text{Si}_{0.55}$, is depicted in Figure 3. In the figure, different T_C values of the same compositions, which depend on the annealing temperature, are also shown. Since the differences in Mn/Fe and P/Si contents between the three series were trivial, the Curie temperature was mainly determined by the Ru content. Roughly speaking, T_C decreased with increasing the Ru content linearly at a rate of 2.5 K/at. % Ru. This value was much smaller than that of the Co substitution (4.3–6.6 K/at. % Co) or Fe substitution (5.6–8.1 K/at. % Ni) for $(\text{MnFe})_{1.95}\text{P}_{0.5}\text{Si}_{0.5}$ [16]. In this sense, the Ru-substituted system is advantageous for the fine control of T_C by changing the content. The thermal hysteresis estimated from Figure 2 is listed in Table 1. All the compounds have a ΔT_{hys} less than 2 K. Figure 4a,b show the temperature dependence of the magnetic entropy change of $\text{Mn}_{\sim 1.24}\text{Fe}_{\sim 0.76-x}\text{Ru}_x\text{P}_{\sim 0.46}\text{Si}_{\sim 0.54}$ in a field change of 1.5 T. Most of the samples had peak values of the magnetic entropy change, ΔS_{max} , higher than 10 J/K·kg. The ΔS_{max} of samples 5, 8 and 9 exceeded 15 J/K·kg. The half width of the ΔS_M peak was in the range of 4–7 K. On the other hand, the difference in T_C between the adjacent sample numbers was, at most, 4 K (see Table 1). Thus, a large overlap of two adjacent $\Delta S_M - T$ curves was observed between the ΔS_M peaks. This means that the temperature range from 280 to 320 K was completely covered by $\text{Mn}_{\sim 1.24}\text{Fe}_{\sim 0.76-x}\text{Ru}_x\text{P}_{\sim 0.46}\text{Si}_{\sim 0.54}$ with large MCEs, which is critical for magnetic refrigerants.

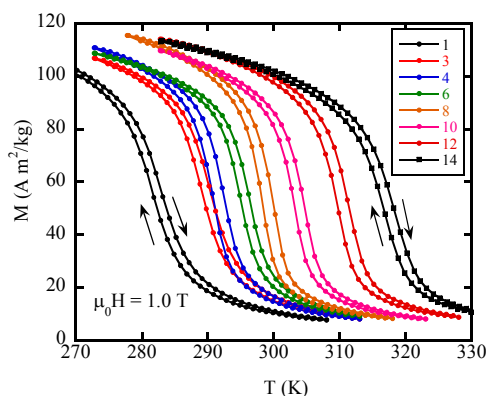


Figure 2. Temperature dependence of magnetization of selected $\text{Mn}_{1.24}\text{Fe}_{0.76-x}\text{Ru}_x\text{P}_{0.46}\text{Si}_{0.54}$ compounds in a magnetic field of 1 T. The numbers represent the sample numbers listed in Table 1. Both heating and cooling processes are plotted.

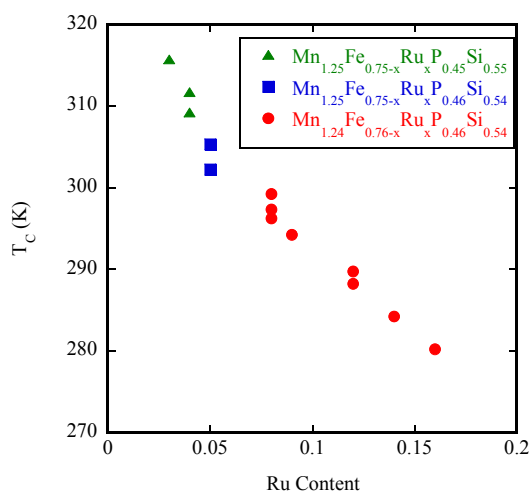


Figure 3. Ru concentration dependence of T_C of three $\text{Mn}_{1.24}\text{Fe}_{0.76-x}\text{Ru}_x\text{P}_{0.46}\text{Si}_{0.54}$ series. The Curie temperature was estimated from the peak position of $dM/dT - T$ curves at 0.2 T in the heating process.

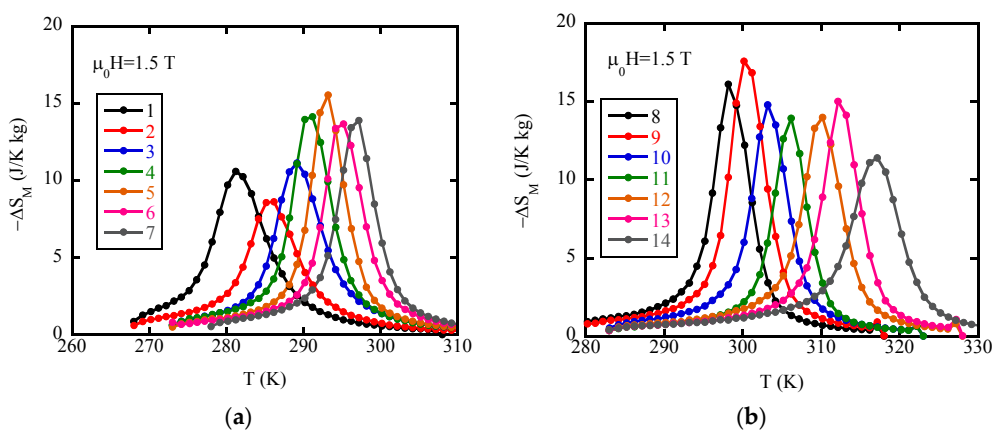


Figure 4. Temperature dependence of the magnetic entropy change of (a) samples No. 1–7 and (b) samples No. 8–14 in field changes of 1.5 T. The numbers represent the sample numbers listed in Table 1. The data were obtained in the heating process.

We calculate the refrigerant capacity of the samples, q , from the following equation,

$$q = \int_{T_C - \delta T}^{T_C + \delta T} |\Delta S_M| dT, \quad (1)$$

where $2\delta T$ is the temperature interval of integration. In the present study, we used $2\delta T = 30$ K. The calculated q values in a field change of 1.5 T are illustrated in Figure 5 by red circles as a function of T_C . Except for a few samples, the q of $\text{Mn}_{-1.24}\text{Fe}_{-0.76-x}\text{Ru}_x\text{P}_{-0.46}\text{Si}_{-0.54}$ was about 115 J/kg. This value is about 1.4 times as large as that of metallic Gd in the same temperature interval. These results also demonstrate the excellent magnetocaloric properties of the Ru-substituted $(\text{MnFe})_2\text{PSi}$ compounds. In Figure 5, the ΔS_{max} values are also plotted by blue squares. In contrast to q , ΔS_{max} shows a broad maximum in the T_C dependence.

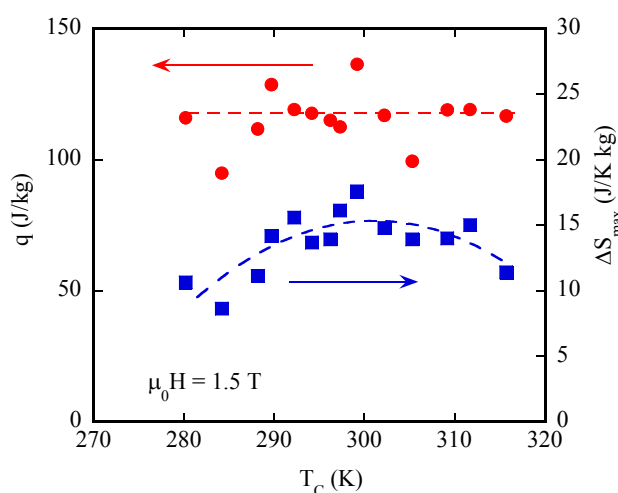


Figure 5. The refrigerant capacity, q , (red circles) at 1.5 T and the peak values of the magnetic entropy change, ΔS_{max} , (blue squares) at 1.5 T of $\text{Mn}_{-1.24}\text{Fe}_{-0.76-x}\text{Ru}_x\text{P}_{-0.46}\text{Si}_{-0.54}$ plotted as a function of the Curie temperature. Dashed lines are guides to the eye.

This is understood as follows. From the Maxwell relation, ΔS_M is expressed as:

$$\Delta S_M = \int_0^H \left(\frac{\partial M}{\partial T} \right)_H dH. \quad (2)$$

Therefore, sharp FOMTs give large ΔS_{max} . As the Curie temperature is raised, the magnetic transition becomes less sharp, because the system approaches the critical boundary for the FOMT. This causes a decrease in ΔS_{max} with the increasing T_C . On the other hand, the magnetic transition becomes broad with the increasing the Ru content, because Ru is a nonmagnetic element. Then, lowering T_C gives rise to a reduction of ΔS_{max} , and, as a result, ΔS_{max} has a maximum at an intermediate T_C . When the magnetic transition is round, the half width of the ΔS_M peak becomes large. Consequently, the refrigerant capacity is constant in the whole temperature range studied.

3. Materials and Methods

The samples were synthesized in the standard procedures: (1) mixing in a ball mill, (2) sintering in the furnace, (3) pulverizing at room temperature, and (4) subsequent annealing. The purity of the raw materials are 3 N for Mn, Fe, and Ru, 4 N for Si, and 6 N for P. Metallic powders and small pieces of P and Si weighted in desired compositions were mixed in a planetary ball mill under Ar atmosphere. The ball milling was carried out for 10 h at a rotational speed of 200 rpm using hardened

stainless steel vials and balls. The resultant was placed in a carbon boat and sintered in a furnace for 5 h. The inside of our furnace tube can be evacuated. Sintering was done under Ar atmosphere. After cooled down to room temperature, the products were pulverized and mixed in a ball mill. Then, the samples were annealed at the same temperature as sintering for 5 h to ensure homogeneity. The procedures (3) and (4) were repeated to improve homogeneity. The amount of one batch is about 70 g in this study. X-ray diffraction measurements were carried out for some samples. The diffraction patterns indicate that the samples have an almost single phase with the Fe₂P-type structure. Very weak peaks due to the impurity phase with the cubic Fe₃Si-type structure were detected. No differences between the X-ray diffraction patterns of the same compositions with different annealing temperature were observed. The differential scanning calorimetry (DSC) measurements were performed using a commercial DSC apparatus, DSC7000X (Hitachi High-Tech Science, Tokyo, Japan) with heating rate of 2 K/min in the temperature range of 243–328 K. The magnetization was measured in a commercial SQUID magnetometer, MPMS-5S (Quantum Design Japan, Tokyo, Japan). The magnetic entropy change, ΔS_M is obtained from the Maxwell relation given in Equation (2). It is important to note that ΔS_M is sometimes overestimated by applying the $M - H$ data to the Maxwell relation, when the material has large thermal hysteresis. This is because some parts of the sample remain in the ferromagnetic state, when a magnetic field is removed at a temperature around T_C . Consequently, both the ferromagnetic and paramagnetic states coexist and the material shows an anomalous $M - H$ curve at an adjacent temperature, giving rise to incorrect ΔS_M . Detailed discussion on this problem is given in the literature [17–19]. In the present study, the $M - T$ curves measured at various fields are used to estimate ΔS_M . Our group confirmed that this method gives correct ΔS_M [20,21]. The sample was cooled down far below T_C in zero field and the $M - T$ curve was recorded in the heating process.

4. Conclusions

We have studied the magnetocaloric properties of Mn_{~1.24}Fe_{~0.76-x}Ru_xP_{~0.46}Si_{~0.54} compounds with $0.03 \leq x \leq 0.16$ and obtained the following conclusions.

- (i) Repetitive annealing improves the homogeneity of the sample and it makes the magnetic transition sharper.
- (ii) We succeeded in the fine control of T_C between 275 and 315 K by changing the Ru content and the sintering temperature. Roughly speaking, T_C is determined by the Ru content and it is decreased by increasing the Ru content nearly linearly at a rate of 2.5 K/at. % Ru in Mn_{~1.24}Fe_{~0.76-x}Ru_xP_{~0.46}Si_{~0.54}.
- (iii) All the compounds undergo the FOMT and exhibit large MCEs with ΔT_{hys} less than 2 K. It was found that the refrigerant capacity is almost constant in the composition ranges studied.

These results indicate that Mn_{~1.24}Fe_{~0.76-x}Ru_xP_{~0.46}Si_{~0.54} compounds are excellent candidates for magnetic refrigerants near room temperature.

Finally, we add supplementary comments on our production process. In the present study, the samples were synthesized by sintering and annealing. This method is advantageous for the production of a large amount of materials at an industrial scale compared with other methods, such as melt spinning or the drop synthesis method. The amount of one sample is about 70 g, which is larger than that prepared by using quartz ampoules in a laboratory. Our samples underwent a sharper FOMT than those synthesized in quartz ampoules. Moreover, we confirmed that the Curie temperature is reproducible within ± 1 K when the samples are prepared with the same initial compositions and the same annealing temperature [13]. These results demonstrate that our method gives homogeneous and reliable materials.

Recent magnetic refrigeration systems are based on the active magnetic regenerator (AMR) cycle. In this cycle, a large temperature span can be achieved by adopting the layered structure of several materials. The present study indicates that the Mn_{~1.24}Fe_{~0.76-x}Ru_xP_{~0.46}Si_{~0.54} system offers a large

temperature span from 275 K to 315 K. To test the cooling power, we are mounting the present compounds to the magnetic refrigeration system. The results will be reported in the near future.

Acknowledgments: This work was partially supported by the Advanced Low Carbon Technology Research and Development Program, ALCA, of the Japan Science and Technology Agency, JST.

Author Contributions: Keiichiro Yamashita designed the experiments. Takayuki Ohnishi and Kei Soejima performed the experiments. Hirofumi Wada analyzed the experimental data. All of the authors contributed to discussion and Hirofumi Wada wrote the manuscript.

Conflicts of Interest: The authors declare no conflict of interest.

References

1. Brown, G.V. Magnetic heat pumping near room temperature. *J. Appl. Phys.* **1976**, *47*, 3673–3680. [[CrossRef](#)]
2. Pecharsky, V.K.; Gschneidner, K.A., Jr. Giant magnetocaloric effect in $\text{Gd}_5(\text{Si}_2\text{Ge}_2)$. *Phys. Rev. Lett.* **1997**, *78*, 4494–4497. [[CrossRef](#)]
3. Wada, H.; Tanabe, Y. Giant magnetocaloric effect of $\text{MnAs}_{1-x}\text{Sb}_x$. *Appl. Phys. Lett.* **2001**, *79*, 3302–3304. [[CrossRef](#)]
4. Tegus, O.; Brück, E.; Buschow, K.H.J.; de Boer, F.R. Transition-metal-based magnetic refrigerants for room-temperature applications. *Nature* **2002**, *415*, 150–152. [[CrossRef](#)] [[PubMed](#)]
5. Fujita, A.; Fujieda, S.; Hasegawa, Y.; Fukamichi, K. Itinerant-electron metamagnetic transition and large magnetocaloric effects in $\text{La}(\text{Fe}_x\text{Si}_{1-x})_{13}$ compounds and their hydrides. *Phys. Rev. B* **2003**, *67*, 104416. [[CrossRef](#)]
6. Krenke, T.; Duman, E.; Acet, M.; Wassermann, E.F.; Moya, X.; Manosa, L.; Planes, A. Inverse magnetocaloric effect in ferromagnetic Ni-Mn-Sn alloys. *Nat. Mater.* **2005**, *4*, 450–454. [[CrossRef](#)] [[PubMed](#)]
7. Liu, D.; Yue, M.; Zhang, J.; McQueen, T.M.; Lynn, J.W.; Wang, X.; Chen, Y.; Li, J.; Cava, R.J.; Liu, X.; et al. Origin and tuning of the magnetocaloric effect in the magnetic refrigerant $\text{Mn}_{1.1}\text{Fe}_{0.9}(\text{P}_{0.8}\text{Ge}_{0.2})$. *Phys. Rev. B* **2009**, *79*, 014435. [[CrossRef](#)]
8. Cam Thanh, D.T.; Brück, E.; Trung, N.T.; Klaasse, J.C.P.; Buschow, K.H.J.; Ou, Z.Q.; Tegus, O.; Caron, L. Structure, magnetism, and magnetocaloric properties of $\text{MnFeP}_{1-x}\text{Si}_x$ compounds. *J. Appl. Phys.* **2008**, *103*, 07B318. [[CrossRef](#)]
9. Yue, M.; Li, Z.Q.; Xu, H.; Huang, Q.Z.; Liu, X.B.; Liu, D.M.; Zhang, J.X. Effect of annealing on the structure and magnetic properties of $\text{Mn}_{1.1}\text{Fe}_{0.9}\text{P}_{0.8}\text{Ge}_{0.2}$ compound. *J. Appl. Phys.* **2010**, *107*, 09A939. [[CrossRef](#)]
10. Dung, N.H.; Zhang, L.; Ou, Z.Q.; Brück, E. From first-order magneto-elastic to magneto-structural transition in $(\text{Mn,Fe})_{1.95}\text{P}_{0.50}\text{Si}_{0.50}$ compounds. *Appl. Phys. Lett.* **2011**, *99*, 092511. [[CrossRef](#)]
11. Wada, H.; Nakamura, K.; Katagiri, K.; Ohnishi, T.; Yamashita, K.; Matsushita, A. Tuning the Curie temperature and thermal hysteresis of giant magnetocaloric $(\text{MnFe})_2\text{PX}$ ($X = \text{Ge}$ and Si) compounds by the Ru substitution. *Jpn. J. Appl. Phys.* **2014**, *53*, 063001. [[CrossRef](#)]
12. Brück, E.; Trung, N.T.; Ou, Z.Q.; Buschow, K.H.J. Enhanced magnetocaloric effects and tunable thermal hysteresis in transition metal pnictides. *Scr. Mater.* **2012**, *67*, 590–593. [[CrossRef](#)]
13. Wada, H.; Takahara, T.; Katagiri, K.; Ohnishi, T.; Soejima, K.; Yamashita, K. Recent progress of magnetocaloric effect and magnetic refrigerant materials of Mn compounds. *J. Appl. Phys.* **2015**, *117*, 172606. [[CrossRef](#)]
14. Yu, H.Y.; Zhu, Z.R.; Lai, J.W.; Zheng, Z.G.; Zeng, D.C.; Zhang, J.L. Enhance magnetocaloric effects in $\text{Mn}_{1.15}\text{Fe}_{0.85}\text{P}_{0.52}\text{Si}_{0.45}\text{B}_{0.03}$ alloy achieved by copper-mould casting and annealing treatments. *J. Alloys Compd.* **2015**, *649*, 1043–1047. [[CrossRef](#)]
15. Höglin, V.; Cedervall, J.; Andersson, M.S.; Sarkar, T.; Hudl, M.; Nordblad, P.; Andersson, Y.; Sahlberg, M. Phase diagram, structures and magnetism of the $\text{FeMnP}_{1-x}\text{Si}_x$ -system. *RSC Adv.* **2015**, *5*, 8278–8285. [[CrossRef](#)]
16. Ou, Z.Q. Magnetic Structure and Phase Formation of Magnetocaloric Mn-Fe-P-X Compounds. Ph.D. Thesis, Technische Universiteit Delft, Delft, The Netherlands, 10 July 2013.
17. Balli, M.; Fruchart, D.; Gignoux, D.; Zach, R. The “colossal” magnetocaloric effect in $\text{Mn}_{1-x}\text{Fe}_x\text{As}$: What are we really measuring? *Appl. Phys. Lett.* **2009**, *95*, 072509. [[CrossRef](#)]

18. Quintana-Nedelcos, A.; Sánchez Llamazares, J.L.; Sánchez-Valdés, C.F.; Álvarez Alonso, P.; Gorria, P.; Shamba, P.; Morley, N.A. On the correct estimation of the magnetic entropy change across the magneto-structural transition from the Maxwell relation: Study of MnCoGeB_x alloy ribbons. *J. Alloys Compd.* **2017**, *694*, 1189–1195. [[CrossRef](#)]
19. Caron, L.; Ba Doan, N.; Ranno, L. On entropy change measurements around first order phase transitions in caloric materials. *J. Phys. Condens. Matter* **2017**, *29*, 075401. [[CrossRef](#)] [[PubMed](#)]
20. Wada, H.; Tanabe, Y.; Shiga, M.; Sugawara, H.; Sato, H. Magnetocaloric effects of Laves phase Er(Co_{1-x}Ni_x)₂ compounds. *J. Alloys. Compd.* **2001**, *316*, 245–249. [[CrossRef](#)]
21. Wada, H.; Matsuo, S.; Mitsuda, A. Pressure dependence of magnetic entropy change and magnetic transition in MnAs_{1-x}Sb_x. *Phys. Rev. B* **2009**, *79*, 092407. [[CrossRef](#)]



© 2017 by the authors; licensee MDPI, Basel, Switzerland. This article is an open access article distributed under the terms and conditions of the Creative Commons Attribution (CC BY) license (<http://creativecommons.org/licenses/by/4.0/>).